

Article

Excess Phase Noise Characterization in Multifrequency Remote Clock Distribution Based on Femtosecond Frequency Combs

Changjun Hu ^{1,2,†}, Ravi P. Gollapalli ^{3,†}, Lin Yang ¹ and Lingze Duan ^{1,*}

¹ Department of Physics, University of Alabama in Huntsville, Huntsville, AL 35899, USA; E-Mail: ly0003@uah.edu

² Research Institute of Telecommunications Transmission, Beijing 100191 China; E-Mail: huchangjun@ritt.cn

³ Department of Electrical and Computer Engineering, University of South Alabama, Mobile, AL 36688, USA; E-Mail: gollapalli@southalabama.edu

† These authors contributed equally to this work.

* Author to whom correspondence should be addressed; E-Mail: ld0003@uah.edu; Tel.: +1-256-824-2138; Fax: +1-256-824-6873.

Academic Editor: Takayoshi Kobayashi

Received: 7 March 2015 / Accepted: 28 April 2015 / Published: 7 May 2015

Abstract: Remote distribution of optical frequency references, based on multifrequency sources such as femtosecond frequency combs, holds many advantages over its single-frequency counterpart. However, characterizing the excess noise caused by the transmission links or external perturbations in a multifrequency scheme posts new challenges. We have experimentally demonstrated direct measurement of excess phase noise spectrum in both free-space and fiber-optic transfer of a frequency comb using a multiheterodyne technique. In fiber-optic distribution, we focused on the excess phase noise under a single-tone acoustic perturbation. Increased overall noise power and a change of phase noise spectrum have been observed. In free-space distribution, a fractional instability of 3×10^{-14} at 1 s was observed for a 60 m outdoor atmospheric transmission, and large phase modulation due to air fluctuations causes a sizable line broadening.

Keywords: clock distribution; optical frequency comb; multiheterodyne; phase noise; fiber optics; free-space communication

1. Introduction

Time and frequency distribution is a key enabling technology for remote clock synchronization, which finds applications in telecommunication, navigation, grid deployment, remote sensing, precision measurement, and fundamental research. With the advent of optical atomic clocks [1–4] and their much higher stability over traditional atomic clocks operating at microwave frequencies, it has become increasingly clear that future remote clock synchronization, especially on the backbone level, must be accomplished in the optical domain.

Recently, remote distribution of optical-frequency references has attracted considerable interest [5–19]. There are in general two possible transfer media: *optical fiber* and *free space*. An optical fiber provides a light transfer path isolated from the surrounding environment, minimizing excess noises added to the clock signals during beam propagation and hence maximizing the fidelity of the delivered frequency references. Coherent optical links spanning well over 100 km have been experimentally demonstrated by a number of groups [5–9]. On the other hand, free-space clock distribution benefits from its flexibility and low overhead cost, and has proved to be a feasible option for short-distance, *ad hoc* networks or networks among mobile hubs, despite its much poorer link fidelity due primarily to air turbulence [15–19]. It is also the only option for space-terrestrial network synchronization [17].

So far, most of the effort in both fiber-optic and free-space clock distribution has been devoted to the realization of faithful delivery of a *single-frequency optical carrier* [5–10,15,17]. An alternative approach, meanwhile, transfers *multiple frequency references* simultaneously in the form of an optical frequency comb (OFC) [13,14,16,18,19]. The advantage of the latter scheme rests on its ability to directly synchronize clocks operating at different wavelengths, for example between an Hg⁺ clock and a Ca clock [20], or even in different domains, for example between an optical atomic clock and a traditional atomic clock, such as a Cs clock [1]. As a result, direct distribution of an OFC can potentially suit a broader range of network synchronization scenarios.

One of the most important issues in remote clock distribution is the *excess phase noise*, which refers to the extra phase noise added to the original highly-coherent frequency references by the transfer media due to fluctuations inherent to them or external perturbations. For a multifrequency clock transfer scheme, characterizing the excess phase noise is more challenging because multiple waves are simultaneously involved and the phase noise added by the transfer medium to each wave may not necessarily be the same. On top of that, dispersion could further complicate the problem. Therefore, in general, the instability of a multi-frequency clock transfer link is characterized by the long-term error of the clock (e.g., the Allan deviation) rather than the phase noise spectrum [13]. However, under certain conditions, phase noise can be directly measured in a multifrequency scheme with a well-defined meaning.

We have recently proposed a multiheterodyne technique for direct phase noise characterization of a multifrequency clock distribution system [19]. In essence, multiheterodyne is a generalization of the optical heterodyne technique used for characterizing single-carrier clock distribution systems [14]. It measures the coherent superposition of the optical heterodyne signals generated by multiple frequency components. When the refractive index fluctuation of the transfer medium is small enough so that its impact to all of the involved frequency components can be treated as approximately equal, the multiheterodyne signal becomes a close representation of the optical heterodyne signal produced by individual frequency components [19].

Here we report our experiments on multiheterodyne characterization of the excess phase noise in both fiber-optic and free-space distributions of an OFC. In fiber-optic distribution, we introduced an external, monotone acoustic perturbation and studied its impact on the phase noise spectrum and the total rms noise amplitude. In free-space distribution, we delivered a femtosecond pulse train from an OFC laser across a 60 m rooftop atmospheric link and measured the spectral broadening and phase noise spectra caused by turbulence. Our results demonstrate the effectiveness of multiheterodyne in characterizing the excess phase noise in various settings of multifrequency remote clock transfer.

2. Fiber-Optic Distribution

In the case of fiber-optic clock distribution, the focus of our work is on quantifying the effects of external acoustic perturbations on the phase noise of optical clock signals propagating in a fiber link. The work shares some similarities with the 1992 experiment by Pang *et al.* [21] but focuses on the contemporary topic of fiber-optic remote transfer of an OFC.

2.1. Experimental Setup

In our experiment, we let a frequency comb propagate through a section of fiber and use a loudspeaker to introduce various types of acoustic perturbations to the fiber. We then compare the output from the fiber with the original comb to find out the amount of excess noise. Figure 1 shows a schematic of the experimental setup. The light source is a commercial femtosecond-laser frequency comb (FC1500, Menlo Systems, Martinsried, Germany) operating at 1.56 μm , with comb line spacing (*i.e.*, pulse repetition rate) of 250 MHz. The optical system is essentially a Mach-Zehnder interferometer sandwiched between two fiber couplers. In the signal arm, an erbium-doped fiber amplifier (EDFA-16-LC, Optilab, Phoenix, AZ, USA; EDFA) and a variable optical attenuator (VOA50, Thorlabs, Newton, NJ, USA; VOA) control the signal power to achieve the optimum signal-to-noise ratio while preventing detector saturation. The fiber link consists of a section of either single-mode fiber (SMF-28; SMF) or polarization maintaining fiber (HB1500T; PMF) wound loosely on a plastic spool. For the SMF, two different fiber lengths, 80 m and 800 m, are tested. A loudspeaker is placed a few centimeters away on the side of the spool and is driven by a signal generator. A polarization controller (PC) is inserted after the fiber link to optimize the output signal. In the reference arm, an acousto-optic frequency shifter (AMM-80, Brimrose, Sparks, MD, USA; AOFS) is used to add an 80 MHz offset to the frequencies of the reference signal. The two arms then combine at a fiber coupler, which directs the interferometer output to a photodetector (DET01CFC, Thorlabs, Newton, NJ, USA; PD). The reference arm is only several meters long, significantly shorter than the signal arm. Its length is chosen so that pulses from both arms can temporally overlap on the detector. In addition, the pulse repetition rate of the laser is frequently adjusted around its 250 MHz nominal value through a computerized control system to maintain the optimum pulse overlapping condition. This is because a repetition rate change can cause a change of the relative pulse delay in an imbalanced interferometer [22].

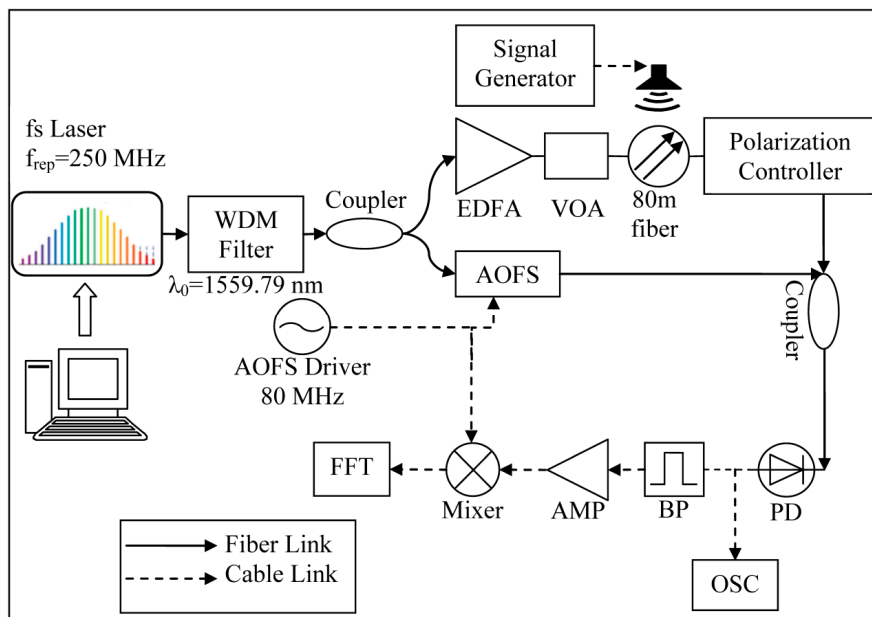


Figure 1. Schematic of the experimental setup for characterizing the excess phase noise spectra of optical frequency transfer in a fiber link under external acoustic perturbations. AMP, microwave amplifier; BP, band pass filter; OSC, oscilloscope; WDM, wavelength division multiplexer.

The beating between the two overlapped pulses generates an 80 MHz beat note on the photodetector. This heterodyne process, however, is complicated by the fact that a frequency comb is composed of a series of discrete spectral lines and the beat note is hence due to multi-heterodyne. A detailed theoretical analysis of multi-heterodyne phase noise detection has been given elsewhere [19]. Here, we just point out that, in order to minimize the impact of fiber dispersion to the heterodyne signal, a narrow band optical filter centered at 1559.79 nm with a pass band of 0.4 nm (*i.e.*, about 100 GHz) is inserted at the output of the laser. The beat note is passed through a bandpass filter and an amplifier before it is mixed in quadrature with the 80 MHz driving signal from the AOFS driver. The resulting dc signal is then frequency analyzed by a fast Fourier transform (FFT) analyzer (SR785, Stanford Research Systems, Sunnyvale, CA, USA) to reveal the noise spectrum. Meanwhile, an oscilloscope (GDS-2204, Instek, Montclair, CA, USA) is used to monitor the 80 MHz beat note in the time domain.

It should be noted that the OFC was in free-run (without stabilization of the pulse repetition rate and the carrier-envelope offset frequency) during the measurements. This is valid in our case because, for excess noise measurements, where both the signal and the reference are derived from the same femtosecond laser, the laser phase noise enters the multiheterodyne beat note as a result of arm-length imbalance in the interferometer. In most of our measurements (for both *fiber-optic* and *free-space* transfer tests), this imbalance is in the order of 100 m, much less than the coherence length of the OFC (a free-run fiber-based OFC typically has a comb-line linewidth of about 20 kHz near its center wavelength [23]). As a result, the impact of the laser noise is negligible compared to the added noise. Moreover, our experience with operating the OFC indicates that stabilizing the OFC with an rf atomic clock, such as a Cs or Rb clock, can dramatically reduce the slow frequency drift of the comb lines,

but does little to improve the short-term linewidth. Therefore, for short-distance demonstrations, a free-run OFC works sufficiently well.

2.2. Experimental Results

In the experiment, we first verify that our detection system can allow us to see the excess phase noise due to pulse propagation in the fiber. This is done by measuring the phase noise at the output of the interferometer with the speaker turned off and with different lengths of SMF inserted in the signal arm. The phase noise is found to be proportional to the fiber length, indicating a direct correlation between the excess phase noise and the fiber. We then focus our attention on the noise behavior under external perturbations.

The simplest way of acoustic perturbation is harmonic perturbation (single-tone). In principle, a more realistic broadband perturbation can be treated as the superposition of many single-tone perturbations. Thus, we focus only on single-tone perturbations in the current study. We have tested two different speaker locations, including putting the speaker on the side of the fiber spool without physical contact and putting it directly on the fiber spool with physical contact. Other than some minor differences in the amplitude, the overall noise spectra follow a similar trend in both cases. Therefore, we only present here the results obtained with the speaker sitting on the side of the fiber spool. Figure 2 shows the excess phase noise spectra with eight different perturbation frequencies. All the data are obtained with an 80 m transmission distance in SMF, and are measured within the span of about 1 hour in normal lab conditions. The driving power to the speaker remains the same for all eight figures. The acoustic power is estimated to be about 80 dB in decibel scale.

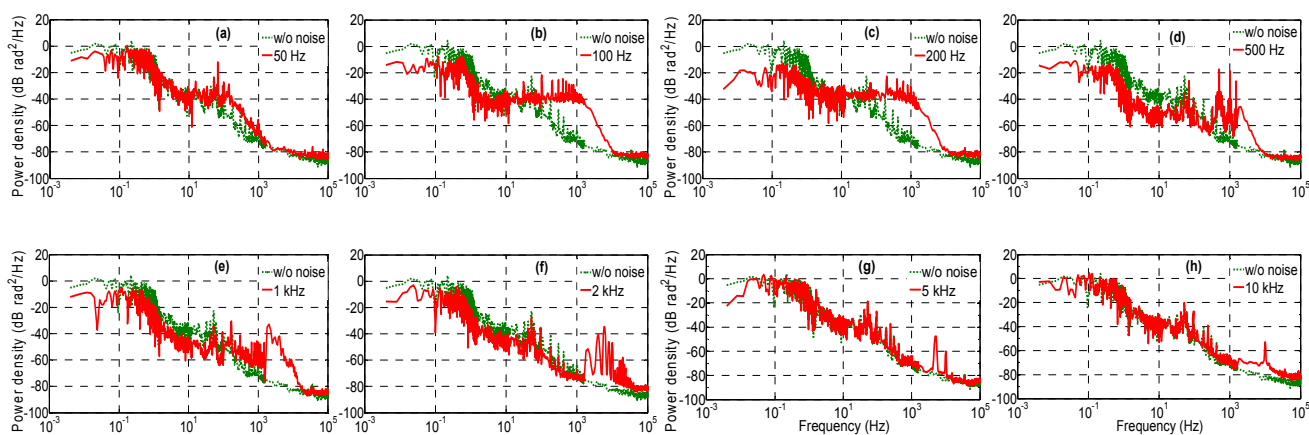


Figure 2. Excess phase noise spectra with (solid) and without (dashed) external acoustic perturbations. Measurement is done with 80 m single-mode fiber (SMF) at eight single-tone perturbation frequencies: (a) 50 Hz; (b) 100 Hz; (c) 200 Hz; (d) 500 Hz; (e) 1 kHz; (f) 2 kHz; (g) 5 kHz; and (h) 10 kHz. The driving power is the same for all the frequencies.

It is evident from Figure 2 that the single-tone perturbations cause an increase of phase noise power density within the spectral range of the perturbation frequency and its first few harmonics. Such a behavior agrees with the commonly accepted notion that external acoustic perturbations to optical fibers induce phase fluctuations in the light propagating through the fiber. What is interesting, according to our measured data, is the simultaneous reduction of the noise spectral density at frequencies below the

perturbation frequency. Such an effect exists within the entire tested frequency span, but is especially pronounced between 100 Hz and 1 kHz. The same test is also done with an 800 m transmission distance, and a similar change of the phase noise spectral shape is observed. The decrease of phase noise at frequencies below the excitation frequency indicates that single-tone acoustic perturbation can effectively suppress low-frequency phase noise. The stronger effect within 100–1000 Hz is likely due to the greater acoustic efficiency of the speaker in this frequency range.

One possible mechanism that can lead to the coupling between acoustic excitation and excess transmission phase noise is polarization fluctuation. Physical vibration of the fiber in an external acoustic field can alter the polarization state of the laser beam, resulting in phase fluctuations due to the fiber birefringence. To find out if the noise suppression is related to polarization, we change the 80 m SMF to 80 m PMF in the signal arm and perform the same test at the same perturbation frequencies. Figure 3 shows the excess phase noise spectra under perturbation frequencies of 100 Hz, 200 Hz, 500 Hz and 1 kHz, respectively, along with the spectrum without the perturbation. Compared to the SMF results at the same frequencies, similar noise suppression is observed at low frequencies even with the PMF. This indicates that it is unlikely the noise suppression effect is due to acoustically excited polarization fluctuation.

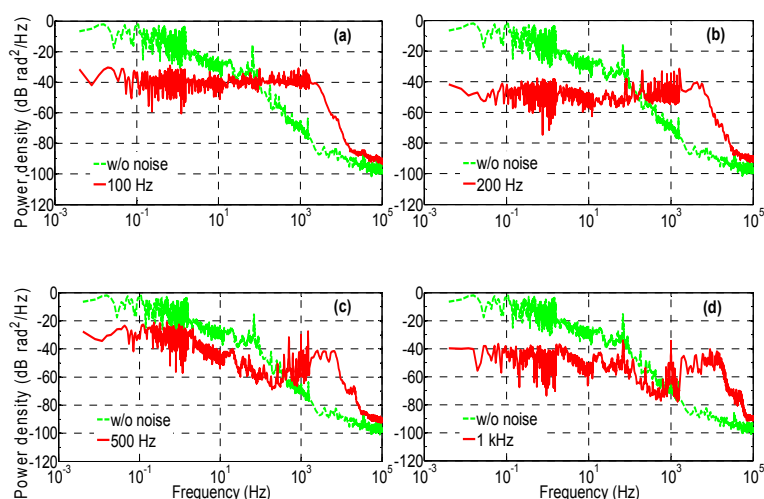


Figure 3. Excess phase noise spectra with (solid) and without (dashed) external acoustic perturbations with 80 m polarization maintaining fiber (PMF) being used. Measurement is done at four single-tone perturbation frequencies: **(a)** 100 Hz; **(b)** 200 Hz; **(c)** 500 Hz; and **(d)** 1 kHz.

Meanwhile, a key question regarding the impact of external excitation is whether single-tone perturbations can cause increase of total phase noise power, which can be calculated by integrating the power spectral density traces in Figures 2 and 3 over the entire frequency span. We compare the total noise powers with and without acoustic perturbations for both SMF and PMF at the four perturbation frequencies between 100 Hz and 1 kHz, where the suppression to low-frequency noise is most significant. The result is summarized in Table 1. Given the noisy nature of the traces, we see some fluctuations in the amount of change of total noise power. But for most cases, the percentage power change with acoustic perturbation range from about 5% to about 10%. Evidently, single-frequency perturbation leads to the increase of phase noise power.

Table 1. Total excess phase noise powers at different perturbation frequencies.

Acoustic Noise Frequency	SMF			PMF		
	Total Noise Power	Absolute Power Change	Percentage Power Change	Total Noise Power	Absolute Power Change	Percentage Power Change
No Perturbation	3.89×10^{-2}	-	-	3.63×10^{-2}	-	-
100 Hz	4.33×10^{-2}	4.37×10^{-3}	11.21%	4.00×10^{-2}	3.76×10^{-3}	10.38%
200 Hz	4.28×10^{-2}	3.84×10^{-3}	9.87%	3.83×10^{-2}	2.06×10^{-3}	5.69%
500 Hz	3.92×10^{-2}	2.07×10^{-4}	0.53%	3.93×10^{-2}	3.02×10^{-3}	8.34%
1 kHz	4.38×10^{-2}	4.84×10^{-3}	12.42%	3.84×10^{-2}	2.11×10^{-3}	5.80%

2.3. Discussion

While the increase of the total noise power under external acoustic excitation is as expected, the suppression of the low-frequency phase noise by a single-tone perturbation is somewhat a surprise. The exact mechanism causing this interesting effect is subject to further investigation. One possible scenario is, when an acoustic wave strikes a fiber, the pressure oscillation in the air prompts periodic changes of strain and stress inside the fiber and hence periodic fluctuations of the refractive index. With sufficient amplitude, the resulting periodic phase variation of light can average out the phase noise caused by spontaneous fluctuations of strain and stress at lower frequencies, leading to a suppression of the noise spectral density below the perturbation frequency. This effect can be stronger in anisotropic fiber structures such as PMFs compared to isotropic structures such as SMFs because the fluctuations of strain and stress are more appreciable in anisotropic structures. Nevertheless, the present work demonstrates experimentally the impact of acoustic perturbations to fiber-optic remote clock distribution and characterizes the excess phase noise spectrum for the frequency comb-based scheme. The noise-suppression effect by single-tone acoustic perturbations potentially offers a way to manipulate the phase noise spectrum of transferred clocks at low frequencies without active noise cancellation.

3. Free-Space Distribution

For free-space clock distribution, because of the much stronger disturbance to the optical beam due to turbulence, there is no need to introduce additional noise. Meanwhile, since air has a much smaller dispersion than fiber, the multiheterodyne bandwidth can potentially be much greater. These two distinctions make the free-space test different from the fiber-optic test.

3.1. Experimental Setup

Figure 4 shows the schematic of the experimental system. The entire setup is located on the rooftop of our laboratory building on the campus of the University of Alabama in Huntsville. A commercial fiber laser (FFL-1560, Precision Photonics, Boulder, CO, USA) acts as the laser source generating a near-infrared (center wavelength 1560 nm) femtosecond pulse train with a 4 mW average power, a 90 MHz pulse repetition rate, and a pulse width of about 150 fs. A highly-doped erbium-doped fiber amplifier developed in house is used to amplify the pulse train to 100 mW average power with the pulsewidth shortened to less than 100 fs. A fiber coupler (AC Photonics, Santa Clara, CA, USA) splits 30% of the power to the reference arm and the remaining power is used for the transmission. For the

purpose of optical heterodyning detection, the reference beam is frequency-shifted by passing it through an acousto-optic modulator (AOM-80, Brimrose, Sparks, MD, USA; AOM) driven at 80 MHz and selecting the first order deflection. It then goes through a tunable delay line, which ensures temporal overlapping of the femtosecond pulses from the reference and the transmission paths. The transmission pulse train is collimated into a 7 mm diameter beam at a fiber collimator and launched into the atmospheric transmission link. The beam is reflected back to the experimental setup by a 2-inch gold mirror housed in a sturdy fixture mounted on the rooftop platform at a distance of 30 m (*i.e.*, 60 m round-trip distance). The collected transmitted beam is resized through a telescope before being collinearly combined with the reference beam at a beam-splitter. When optical pulses in both beams temporally overlap, an 80 MHz beat signal is generated. The beat signal is picked up by a photodiode and then sent to a double-balanced mixer, where it is compared to a local oscillator drawn from the original 80 MHz signal driving the AOM. The local signal acquires a slight frequency offset (500 kHz) from 80 MHz at a single-sideband modulator (SSBM). As a result, a 500-kHz beat note is generated by the mixer. It is then sent to a fast Fourier transform (FFT) analyzer (SR785, Stanford Research Systems, Sunnyvale, CA, USA) for a direct measurement of the noise spectrum and a frequency counter for the measurement of the Allan deviation.

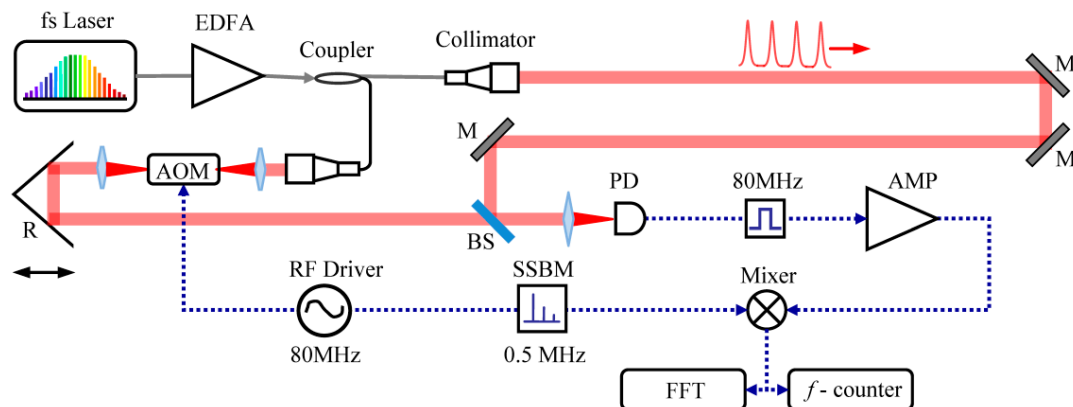


Figure 4. Schematic of the outdoor optical frequency transmission test system. AMP: microwave amplifiers, AOM: acousto-optic modulator, BS: beam splitter, EDFA: erbium-doped fiber amplifier, M: silver mirrors, PD: photodiode, R: retro-reflector, and SSBM: single-side band modulator.

3.2. Experimental Results

The transmission test has been performed at different times of the day and under various weather conditions. Except very windy days, where the laser beam suffers strong beam wander, the noise measurement has given consistent results. Compared to fiber-optic distribution, the magnitude of the excess phase noise for free-space transfer is much greater. This fact can be clearly seen by turning off the SSBM and compare the recovered 80 MHz beat signal directly with the original 80 MHz clock signal driving the AOM. Figure 5a inset shows a time-domain trace of the IF output of the mixer (upon low-pass filtering). It is apparent that the phase fluctuation due to atmospheric propagation is much greater than 2π . This is attributed to the much greater refractive index fluctuation in the air due to turbulence. For such large phase modulations, the direct phase noise measurement scheme used in

fiber-optic distribution is no longer valid. Instead, one has to look at the entire noise sideband of the clock signal to gain a proper evaluation of the phase noise. For this purpose, we directly measured the spectrum of the 500 kHz beat note. Figure 5a shows a typical spectral trace centered at the nominal frequency. The trace is averaged over 1 s. It shows that the optical clock signal is broadened to the scale of hundreds of Hz through the 60 m atmospheric transmission. Such a significant line broadening is believed to be caused by the fluctuation of the refractive index of the air over the transmission path due to wind and turbulence, which works effectively as a phase modulator.

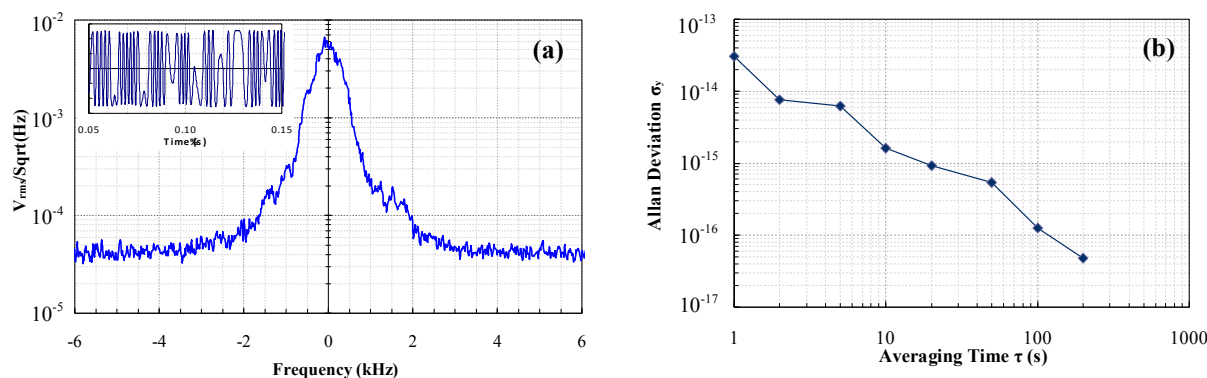


Figure 5. (a) A typical spectrum of the transmission-broadened optical clock signal. Inset: a time-domain trace of the beat note between the recovered clock and the original clock; (b) A typical Allan deviation measurement result.

A typical result of the Allan deviation measurement is shown in Figure 5b. The fractional frequency instability due to transmission is about 3×10^{-14} at 1 s. Considering the difference of the total transmission distance, our results approximately agree with a recent report on optical frequency transfer over a 100 m atmospheric link using a single-frequency laser [15]. The power law of the Allan deviation appears to be close to τ^{-1} , showing possible influence from a white phase or Flicker phase modulation.

4. Conclusions

In conclusion, we have experimentally demonstrated remote distribution of multifrequency optical frequency references via both a fiber-optic and a free-space transfer links. Using a multiheterodyne technique, we have characterized the excess phase noise introduced to the clock signals by the transfer links. In the case of fiber-optic distribution, a single-tone, external acoustic perturbation is introduced and its impact on the phase noise spectrum is studied. Enhancement of noise power is found at the perturbation frequencies and their harmonics, whereas, for a wide span of perturbation frequencies (100–1000 Hz), noise suppression is observed at frequencies below the perturbation frequencies. In the case of free-space distribution, spectral broadening is observed after a 60 m atmospheric transmission and the resulted clock instability is characterized by an Allan deviation measurement. Overall, this research shows the effectiveness of multiheterodyne in the characterization of multifrequency remote clock distribution based on frequency combs.

Acknowledgments

This research is supported in part by the National Science Foundation (ECCS-1040019) and China Scholarship Council (2011307192).

Author Contributions

Hu performed the fiber-optic distribution test and analyzed the data. Gollapalli performed the free-space distribution test and analyzed the data. Yang was the operator of the FC1500 frequency comb laser and was also involved in setting up the fiber-optic experiment. Duan developed the research plan and supervised the entire project.

Conflicts of Interest

The authors declare no conflict of interest.

References

1. Oskay, W.H.; Diddams, S.A.; Donley, E.A.; Fortier, T.M.; Heavner, T.P.; Hollberg, L.; Itano, W.M.; Jefferts, S.R.; Delaney, M.J.; Kim, K.; *et al.* Single-atom optical clock with high accuracy. *Phys. Rev. Lett.* **2006**, *97*, 020801.
2. Rosenband, T.; Hume, D.B.; Schmidt, P.O.; Chou, C.W.; Brusch, A.; Lorini, L.; Oskay, W.H.; Drullinger, R.E.; Fortier, T.M.; Stalnaker, J.E.; *et al.* Frequency ratio of Al⁺ and Hg⁺ single-ion optical clocks; metrology at the 17th decimal place. *Science* **2008**, *319*, 1808–1812.
3. Hinkley, N.; Sherman, J.A.; Phillips, N.B.; Schioppo, M.; Lemke, N.D.; Beloy, K.; Pizzocaro, M.; Oates, C.W.; Ludlow, A.D. An atomic clock with 10⁻¹⁸ instability. *Science* **2013**, *341*, 1215–1218.
4. Bloom, B.J.; Nicholson, T.L.; Williams, J.R.; Campbell, S.L.; Bishof, M.; Zhang, X.; Zhang, W.; Bromley, S.L.; Ye, J. An optical lattice clock with accuracy and stability at the 10⁻¹⁸ level. *Nature* **2014**, *506*, 71–75.
5. Williams, P.A.; Swann, W.C.; Newbury, N.R. High-stability transfer of an optical frequency over long fiber-optic links. *J. Opt. Soc. Am. B* **2008**, *25*, 1284–1293.
6. Musha, M.; Hong, F.; Nakagawa, K.; Ueda, K. Coherent optical frequency transfer over 50 km physical distance using a 120 km-long installed telecom fiber network. *Opt. Express* **2008**, *16*, 16459–16466.
7. Jiang, H.; Kéfélian, F.; Crane, S.; Lopez, O.; Lours, M.; Millo, J.; Holleville, D.; Lemonde, P.; Chardonnet, C.; Amy-Klein, A.; *et al.* Long-distance frequency transfer over an urban fiber link using optical phase stabilization. *J. Opt. Soc. Am. B* **2008**, *25*, 2029–2035.
8. Grosche, G.; Terra, O.; Predehl, K.; Holzwarth, R.; Lipphardt, B.; Vogt, F.; Sterr, U.; Schnatz, H. Optical frequency transfer via 146 km fiber link with 10⁻¹⁹ relative accuracy. *Opt. Lett.* **2009**, *34*, 2270–2272.
9. Predehl, K.; Grosche, G.; Raupach, S.M.F.; Droste, S.; Terra, O.; Alnis, J.; Legero, T.; Hänsch, T.W.; Udem, T.; Holzwarth, R.; *et al.* A 920-kilometer optical fiber link for frequency metrology at the 19th decimal place. *Science* **2012**, *336*, 441–444.

10. Fujieda, M.; Kumagai, M.; Gotoh, T.; Hosokawa, M. Ultrastable frequency dissemination via optical fiber at NICT. *IEEE Trans. Instrum. Meas.* **2009**, *58*, 1223–1228.
11. Marra, G.; Slavik, R.; Margolis, H.S.; Lea, S.N.; Petropoulos, P.; Richardson, D.J.; Gill, P. High-resolution microwave frequency transfer over an 86 km-long optical fiber network using a mode-locked laser. *Opt. Lett.* **2011**, *36*, 511–513.
12. Lopez, O.; Amy-Klein, A.; Daussy, C.; Chardonnet, C.; Narbonneau, F.; Lours, M.; Santarelli, G. 86-km optical link with a resolution of 2×10^{-18} for RF frequency transfer. *Euro. Phys. J. D* **2008**, *48*, 35–41.
13. Holman, K.W.; Jones, D.J.; Hudson, D.D.; Ye, J. Precise frequency transfer through a fiber network by use of 1.5 μm mode-locked sources. *Opt. Lett.* **2004**, *29*, 1554–1556.
14. Foreman, S.M.; Holman, K.W.; Hudson, D.D.; Jones, D.J.; Ye, J. Remote transfer of ultrastable frequency references via fiber networks. *Rev. Sci. Instrum.* **2007**, *78*, 021101.
15. Sprenger, B.; Zhang, J.; Lu, Z.H.; Wang, L.J. Atmospheric transfer of optical and radio frequency clock signals. *Opt. Lett.* **2009**, *34*, 965–967.
16. Alatawi, A.; Gollapalli, R.P.; Duan, L. Radio frequency clock delivery via free-space frequency comb transmission. *Opt. Lett.* **2009**, *34*, 3346–3348.
17. Djerroud, K.; Acef, O.; Clairon, A.; Lemonde, P.; Man, C.N.; Samain, E.; Wolf, P. Coherent optical link through the turbulent atmosphere. *Opt. Lett.* **2010**, *35*, 1479–1481.
18. Gollapalli, R.P.; Duan, L. Atmospheric timing transfer using a femto-second frequency comb. *IEEE Photon. J.* **2010**, *2*, 904–910.
19. Gollapalli, R.P.; Duan, L. Multiheterodyne characterization of excess phase noise in atmospheric transfer of a femtosecond-laser frequency comb. *J. Lightwave Technol.* **2011**, *29*, 3401–3407.
20. Udem, T.; Diddams, S.A.; Vogel, K.R.; Oates, C.W.; Curtis, E.A.; Lee, W.D.; Itano, W.M.; Drullinger, R.E.; Bergquist, J.C.; Hollberg, L. Absolute frequency measurements of the Hg and Ca optical clock transitions with a femtosecond laser. *Phys. Rev. Lett.* **2001**, *86*, 4996–4999.
21. Pang, Y.; Hamilton, J.J.; Richard, J. Frequency noise induced by fiber perturbations in a fiber-linked stabilized laser. *Appl. Opt.* **1992**, *31*, 7532–7534.
22. Yang, L.; Nie, J.; Duan, L. Dynamic optical sampling by cavity tuning and its application in lidar. *Opt. Express* **2013**, *21*, 3850–3860.
23. Newbury, N.R.; Swann, W.C. Low-noise fiber-laser frequency combs. *J. Opt. Soc. Am. B* **2007**, *24*, 1756–1770.